DOI: https://doi.org/10.2138/am-2023-9262. http://www.minsocam.org/

Word Count: 2,851

Raman Spectroscopy of the Ilmentite – Geikielite Solid Solution

Laura B. Breitenfeld[1], M. Darby Dyar[2,3], Leif Tokle[4], and Kevin Robertson[5]

[1]Department of Earth and Environmental Science, Wesleyan University, Middletown, CT, USA

[2]Department of Astronomy, Mount Holyoke College, South Hadley, MA, USA

[3]Planetary Science Institute, Tucson, AZ, USA

[4]Department of Earth Sciences, ETH Zürich, Zürich, Switzerland

[5]Deptartment of Earth, Environmental, and Planetary Sciences, Brown University, Providence, RI, USA

Revision 1

Abstract

Ilmenite ($Fe^{2+}TiO_3$) and geikielite ($MgTiO_3$) are important terrestrial minerals relevant to the geology of the Earth, the Moon, Mars, and meteorite samples. Raman spectroscopy is a powerful technique that allows for mineral cation determination for the ilmenite – geikielite solid solution. We report on a sample suite of nine samples within the ilmenite – geikielite solid solution and provide context for their quantitative interpretation. We compare a univariate Raman peak position model for predicting ilmenite composition with a multivariate machine learning model. The univariate model is currently recommended, though the multivariate model may become superior if the data set size is increased. This study lays the groundwork for quantifying Fe (ilmenite) and Mg (geikielite) within oxides minerals using a cheap, portable, and efficient technology like Raman spectroscopy.

Key Words: ilmenite, geikielite, Raman spectroscopy

Introduction

Ilmenite is an important mineral group on planetary surfaces, especially for Earth, the Moon (e.g., Papike et al., 1976; Papike et al., 1991; Lemelin et al., 2013; Surkov et al., 2020), and Mars (e.g., Morris et al., 2006). This group of minerals is also found in a variety of meteorite samples (e.g., Snetsinger and Keil, 1969; Bunch and Keil, 1971). Ilmenite group minerals occur in all rock types, making their study broadly relevant. They are mined on Earth as an important resource material. Most terrestrial occurrences are Fe-rich with the exception of kimberlites, where Mg substitutions exist, acting as a kimberlite indicator (e.g., Wyatt et al., 2004). Lunar ilmenite can have Mg substitutions along the ilmenite – geikielite solid solution (e.g., Papike et al., 1991; Tokle and Robertson, 2019; Robertson et al., 2022). Raman spectroscopy may act as an important tool in the upcoming decades for lunar exploration (e.g., Cloutis et al., 2022) for mineral identification and quantification. Notably, ilmenite group minerals provide information about lunar magmatic evolution (e.g., Sato et al., 2017) that affect interpretations of the Moon's interior. The presence of ilmenite in the SNC (shergottites, nakhlites, chassignites) meteorites is of note in regard to Mars (McSween, 1994; Rull et al., 2004; Wang et al., 2004). Ilmenite group minerals contain valuable compositional information relevant to oxygen fugacity and mineral stability (e.g., see Szymanski et al. (2010) for applicability to Mars). Overall, characterizing the composition of ilmenite on Earth and remote planetary bodies informs geologic interpretations and resource identification (e.g., Heiken and Vaniman, 1990).

There is a solid solution between ilmenite ($Fe^{2+}TiO_3$) and geikielite ($MgTiO_3$), as well as with other minerals like pyrophanite ($MnTiO_3$) at high temperatures. Here, Raman spectroscopy is used to measure the composition of synthetic samples covering the solid solution between ilmenite and geikielite. The cation ratio of Fe to Mg (%ilmenite= (100 × Fe)/(Mg + Fe)) affects positions of the Raman peaks, allowing for the prediction of the mineral compositions. This investigation lays the groundwork for quantifying the cation ratio for the ilmenite – geikielite solid solution using Raman spectroscopy.

Background

Ilmenite and geikielite have three acoustic modes and 27 optical modes. Of these, 10 major Raman spectroscopy bands for ilmenite group minerals occur in the common measurement range from 200 to 800 cm^{-1}. These Raman features are caused by the combination of 5A_g and 5E_g modes (Tibshirani, 1995; Okada et al., 2008). One of the A_g bands, located between ~681 – 715 cm^{-1}, is primarily utilized here.

This work builds on previous studies focused on X-ray diffraction and visible and near-infrared calibrations for the ilmenite – geikielite solid solution using many of the same samples (Tokle et al., 2018; Tokle and Robertson, 2019). Electron microprobe and X-ray diffraction are important tools for distinguishing the mineralogy of the ilmenite – geikielite solid solution. Our well-characterized synthetic mineral samples provide a unique opportunity to evaluate compositional differences within the ilmenite mineral group using Raman spectroscopy, a more accessible and less expensive tool.

Over the last 50 years, a wide variety of studies investigated ilmenite minerals using Raman spectroscopy. Early work included Raman spectral measurements and identification of peak positions (e.g., Beattie and Gilson, 1970; White, 1975; Pinet et al., 1986). Subsequent studies investigate ilmenite properties using Raman spectroscopy like heat capacity and mineral stability (McMillan and Ross, 1987; Chopelas, 1999; Linton and Navrotsky, 1999). Additional research of ilmenite group minerals focused on high-pressure experiments (e.g., Reynard and Guyot, 1994; Okada et al., 2008). Part of the motivation behind these studies is the structural similarity of ilmenites and materials like $MgSiO_3$–ilmenite that are relevant to Earth's mantle.

Raman spectroscopy is useful for applied geologic investigations like geikielite exsolution in spinel (Reusser et al., 2001) and ilmenite detection in Martian meteorites (Wang et al., 2004). Wang et al. (2004) established a correlation between the Raman A_g peak positions (~681 – 715 cm^{-1}) to %ilmenite content in a set of ilmenite – geikielite samples, providing a framework for our investigation.

Methods

All nine synthetic ilmenite and geikielite powders utilized in this study were synthesized from oxides in a 1 atmosphere $CO{:}CO_2$ furnace. Details on the mineral synthesis of these samples are provided in Tokle and Robertson (2019). All powders were sieved to a grain size fraction of 10 – 20 μm. Microprobe analysis shows impurities in all powders are < 1 weight% and chemically homogeneous (Tokle et al., 2018). The electron microprobe analysis values are provided in Table 1 of Tokle and Robertson (2019). The nine samples within the suite include pure ilmenite and geikielite as well as samples compositionally between these end-members (1%, 5%, 10%, 20%, 40%, 60%, and 80% ilmenite). Compared to the natural samples used by Wang et al. (2004), the Mg-rich samples with narrow compositional gaps augment existing Raman data.

Raman spectra were acquired on a Bruker BRAVO Raman dual laser (785 and 852 nm) spectrometer with a spot size of 2 mm in diameter and fixed laser power that did not exceed 100 mW to reduce the risk of material alteration. Five sample scans and an integration time of 10 seconds were utilized at a spectral resolution of 2.0 cm^{-1}/channel.

Univariate data analysis included gaussian peak fitting for the diagnostic ilmenite feature located between ~681 – 715 cm^{-1} (A_g). A linear model was used to fit the univariate Raman peak position data when regressed against composition. Partial least squares (PLS) regression, a multivariate machine learning model, was also used to predict %ilmenite content. The PLS method regresses one response variable (%ilmenite) against multiple explanatory variables (intensity at each channel of the spectra), assigning coefficients to every channel (Geladi and Kowalski, 1986; Wold et al., 1983; Wold et al., 2001). Multivariate techniques can exploit broad spectral ranges including multiple diagnostic Raman peaks and do not depend on any single feature's position.

For the univariate and multivariate methods, R^2 values, internal root-mean-square error (RMSE) values, and cross-validated RMSE (RMSE-CV) statistics are reported. RMSE-CV values were calculated by creating three folds of data (square root of the total number of samples) and building a prediction model with the remaining data, then averaging the resultant errors. Here, the RMSE-CV value represent the most accurate prediction error associated with data outside the models. Internal RMSE values allow for comparisons to the literature however, these values underestimate the error of predicting data outside the model. All the RMSE values are in units of %ilmenite.

Results

Seven of the previously reported (e.g., Linton and Navrotsky, 1999; Wang et al., 2004) Raman peaks were directly observed (Figure 1) (Breitenfeld et al., 2023). The geikielite spectrum (purple) has bands at roughly 306, 327, 352, 397, 485, 640, and 715 cm^{-1} (**Table 1**). Raman features of pure ilmenite (yellow) shift to lower wavenumber positions as Fe increases, although several bands are absent or poorly resolved.

Figure 2 depicts the univariate model for predicting %ilmenite using the diagnostic Raman peak position between ~681 – 715 cm^{-1} (A_g) with error bars from the peak fitting. The linear equation from the univariate model results in an R^2 value of 0.99 with internal RMSE and RMSE-CV values equivalent to ±3.9 and ±11.0 %ilmenite, respectively.

Figure 3 shows the internal RMSE and RMSE-CV values for multivariate models with varying numbers of PLS components. The lowest RMSE-CV value is associated with a four component PLS model. However, the small spectral dataset size and large difference between the internal RMSE and RMSE-CV values may indicate that these PLS multivariate models are overfitting the small data set. Overall, all RMSE-CV values for the PLS models are larger (worse) than those for the univariate Raman peak position method.

Discussion

Fewer Raman features are observed for the pure ilmenite sample compared to the pure geikielite sample (**Table 1**). This is consistent with other Raman measurements of these minerals (e.g., Wang et al., 2004). Equivalent to geikielite, 10 Raman modes (5 A_g and 5 E_g) are predicted for ilmenite (Ross and McMillan, 1984). We are interested in understanding this difference in Raman spectral expression further.

Raman spectroscopy allows for the quantification of Fe to Mg within the ilmenite – geikielite solid solution. The reported univariate peak position method outperforms the multivariate PLS method for the current data set size. The Raman peak position of the ilmenite A_g feature between ~681 – 715 cm^{-1} should thus be used to predict the ilmenite and geikielite content of unknown samples.

It must be cautioned that the reported errors (internal RMSE and RMSE-CV) apply only to analyses of ilmenites under these analytical conditions and will likely not be directly comparable to data from different Raman instruments. The effect of predicting the %ilmenite content for natural samples with more diverse cations rather than the pure synthetic samples must also be examined.

A larger sample suite should improve the multivariate model, as observed in other types of spectroscopic investigations (e.g., Dyar and Ytsma, 2021). This work lays the groundwork for an improved multivariate model that exploits valuable spectroscopic information beyond a single Raman feature.

Implications

Raman spectroscopy is a useful tool for mineral identification and quantification. Sample characterization can be performed through cation ratio determinations. This work will aid future workers in answering specific geologic questions related to the ilmenite – geikielite solid solution and relevant applications. For example, inquiries may be pursued related to ilmenite and geikielite mineral associations, alteration conditions, and resource identifications.

Ilmenite is an important mineral group for many planetary bodies including Earth, the Moon, and Mars. This work is particularly relevant to the characterization of terrestrial kimberlites and lunar basalts. In addition to laboratory analyses of terrestrial and extraterrestrial samples, this work is also applicable to handheld Raman spectroscopy measurements. This can be particularly useful for real-time terrestrial field work or planetary surface exploration by astronauts.

Acknowledgments

We are grateful to the NASA SSERVI RIS^{4}E and RISE2 nodes for their support. Thank you to Professor Steven Jaret and the other reviewer for their insightful feedback that improved the quality of this work.

Data Availability

The Raman spectral data are archived in an external data repository at https://zenodo.org/records/10210991 (Breitenfeld et al., 2023).

References

Beattie, I. R., & Gilson, T. R. (1970). The single-crystal Raman spectra of nearly opaque materials. Iron (III) oxide and chromium (III) oxide. *Journal of the Chemical Society A: Inorganic, Physical, Theoretical*, 980-986.

Breitenfeld, L. B., Dyar, M. D., Tokle, L., and Robertson, K. (2023) Raman Spectroscopy of the Ilmenite – Geikielite Solid Solution [Data set] Zenodo. https://zenodo.org/records/10210991.

Bunch, T. E., & Keil, K. (1971). Chromite and ilmenite in non chondritic meteorites. *American Mineralogist: Journal of Earth and Planetary Materials*, *56*(1-2), 146-157.

Chopelas, A. (1999). Estimates of mantle relevant Clapeyron slopes in the MgSiO3 system from high-pressure spectroscopic data. *American Mineralogist*, *84*(3), 233-244.

Cloutis, E. A., Caudill, C., Lalla, E. A., Newman, J., Daly, M., Lymer, E., ... & Wolf, Z. U. (2022). LunaR: Overview of a versatile Raman spectrometer for lunar exploration. *Frontiers in Astronomy and Space Sciences*, *9*, 1016359.

Dyar, M. D., & Ytsma, C. R. (2021). Effect of data set size on geochemical quantification accuracy with laser-induced breakdown spectroscopy. *Spectrochimica Acta Part B: Atomic Spectroscopy*, *177*, 106073.

Geladi, P., and Kowalski, B.R. (1986). Partial least-squares regression: a tutorial. Analytica chimica acta, 185, 1-17.

Heiken, G. H., & Vaniman, D. T. (1990). Characterization of lunar ilmenite resources. In *IN: Lunar and Planetary Science Conference, 20th, Houston, TX, Mar. 13-17, 1989, Proceedings (A90-33456 14-91).*

Lemelin, M., Morisset, C. E., Germain, M., Hipkin, V., Goïta, K., & Lucey, P. G. (2013). Ilmenite mapping of the lunar regolith over Mare Australe and Mare Ingenii regions: An optimized multisource approach based on Hapke radiative transfer theory. *Journal of Geophysical Research: Planets*, *118*(12), 2582-2593.

Linton, J. A., Fei, Y., & Navrotsky, A. (1999). The $MgTiO_3$-$FeTiO_3$ join at high pressure and temperature. *American Mineralogist*, *84*(10), 1595-1603.

McMillan, P. F., & Ross, N. L. (1987). Heat capacity calculations for Al 2 O 3 corundum and MgSiO 3 ilmenite. *Physics and Chemistry of Minerals*, *14*, 225-234.

McSween Jr, H. Y. (1994). What we have learned about Mars from SNC meteorites. *Meteoritics*, *29*(6), 757-779.

Morris, R. V., Klingelhoefer, G., Schröder, C., Rodionov, D. S., Yen, A., Ming, D. W., ... & Arvidson, R. E. (2006). Mössbauer mineralogy of rock, soil, and dust at Gusev crater, Mars: Spirit's journey through weakly altered olivine basalt on the plains and pervasively altered basalt in the Columbia Hills. *Journal of Geophysical Research: Planets*, *111*(E2).

Okada, T., Narita, T., Nagai, T., & Yamanaka, T. (2008). Comparative Raman spectroscopic study on ilmenite-type MgSiO3 (akimotoite), MgGeO3, and MgTiO3 (geikielite) at high temperatures and high pressures. *American Mineralogist*, *93*(1), 39-47.

Papike, J. J., Hodges, F. N., Bence, A. E., Cameron, M., & Rhodes, J. M. (1976). Mare basalts: Crystal chemistry, mineralogy, and petrology. *Reviews of Geophysics*, *14*(4), 475-540.

Papike, J., Taylor, L., & Simon, S. (1991). Lunar minerals. *Lunar sourcebook: A user's guide to the Moon*, 121-181.

Pinet, M., Smith, D. C., & Boyer, H. (1986). Raman fingerprinting of opaque and semi-opaque minerals: the natural system Geikielite-ilmenite-pyrophanite (GIP). *Terra Cognita*, *7*, 18.

Reusser, E., Gieré, R., & Lumpkin, G. R. (2001). Geikielite exsolution in spinel. *American Mineralogist*, *86*(11-12), 1435-1446.

Reynard, B., & Guyot, F. (1994). High-temperature properties of geikielite (MgTiO3-ilmenite) from high-temperature high-pressure Raman spectroscopy—some implications for MgSiO3-ilmenite. *Physics and Chemistry of Minerals*, *21*(7), 441-450.

Robertson, K., Milliken, R., Pieters, C., Tokle, L., Cheek, L., & Isaacson, P. (2022). Textural and compositional effects of ilmenite on the spectra of high-titanium lunar basalts. *Icarus*, *375*, 114836.

Ross, N. L., & McMillan, P. (1984). The Raman spectrum of MgSiO3 ilmenite. *American Mineralogist*, *69*(7-8), 719-721.

Rull, F., Martinez-Frias, J., Sansano, A., Medina, J., & Edwards, H. G. M. (2004). Comparative micro-Raman study of the Nakhla and Vaca Muerta meteorites. *Journal of Raman Spectroscopy*, *35*(6), 497-503.

Sato, H., Robinson, M. S., Lawrence, S. J., Denevi, B. W., Hapke, B., Jolliff, B. L., & Hiesinger, H. (2017). Lunar mare TiO2 abundances estimated from UV/Vis reflectance. *Icarus*, *296*, 216-238.

Snetsinger, K. G., & Keil, K. (1969). Ilmenite in ordinary chondrites. *American Mineralogist: Journal of Earth and Planetary Materials*, *54*(5-6), 780-786.

Surkov, Y., Shkuratov, Y., Kaydash, V., Korokhin, V., & Videen, G. (2020). Lunar ilmenite content as assessed by improved Chandrayaan-1 M3 data. *Icarus*, *341*, 113661.

Szymanski, A., Brenker, F. E., Palme, H., & El Goresy, A. (2010). High oxidation state during formation of Martian nakhlites. *Meteoritics & Planetary Science*, *45*(1), 21-31.

Tibshirani, R. (1996). Regression shrinkage and selection via the lasso. *Journal of the Royal Statistical Society Series B: Statistical Methodology*, *58*(1), 267-288.

Tokle, L., Robertson, K. M., & Milliken, R. E. (2018). Development of an Fe-Mg Compositional Calibration for the Ilmenite—Geikielite Solid-Solution Using XRD and Reflective Spectroscopy, 49, 2083, 2095.

Tokle, L., & Robertson, K. M. (2019). X-ray diffraction calibration of the Fe^{2+}–Mg^{2+} solid solution of ilmenite, with application to lunar basalts. *European Journal of Mineralogy*, *31*(3), 473-483.

Wang, A., Kuebler, K. E., Jolliff, B. L., & Haskin, L. A. (2004). Raman spectroscopy of Fe-Ti-Cr-oxides, case study: Martian meteorite EETA79001. *American Mineralogist*, *89*(5-6), 665-680.

White, W. B. (1975). Structural interpretation of lunar and terrestrial minerals by Raman spectroscopy. *Infrared and Raman spectroscopy of Lunar and terrestrial minerals*, 325-358.

Wold, S., Martens, H., and Wold, H. (1983). The multivariate calibration problem in chemistry solved by the PLS method. Lecture Notes in Mathematics, 973, 286–293.

Wold, S., Sjöström, M., and Eriksson, L. (2001). PLS-regression: a basic tool of chemometrics. Chemometrics and intelligent laboratory systems, 58(2), 109-130.

Wyatt, B. A., Baumgartner, M., Anckar, E., & Grutter, H. (2004). Compositional classification of "kimberlitic" and "non-kimberlitic" ilmenite. *Lithos*, *77*(1-4), 819-840.

DOI: https://doi.org/10.2138/am-2023-9262. http://www.minsocam.org/

List of Figure Captions

Figure 1. Ilmenite and geikielite Raman spectra acquired on Bruker's BRAVO spectrometer. Spectra are color-coded based on %ilmenite content, where pure $Fe^{2+}TiO_3$ is represented with yellow and pure $MgTiO_3$ with purple.

Figure 2. Univariate model of %ilmenite versus Raman peak position (cm^{-1}) of the diagnostic Raman feature between ~681 – 715 cm^{-1} (A_g) with error bars of the gaussian peak fit. The linear model, R^2 value, internal RMSE, and RMSE-CV are reported.

Figure 3. Multivariate model errors (internal RMSE and RMSE-CV) for 2 – 6 PLS model components.

Figures and Tables

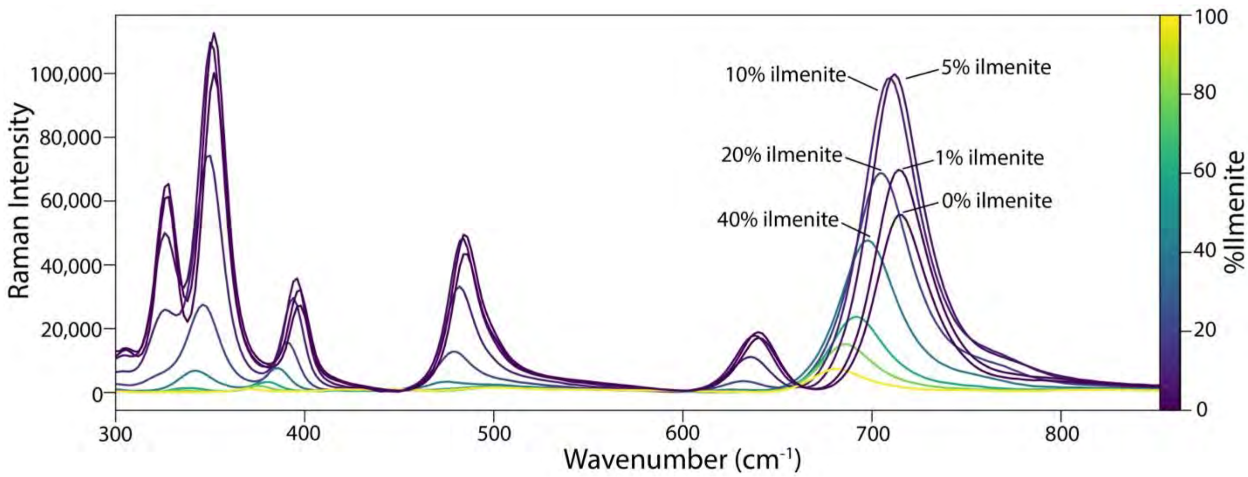

Figure 1. Ilmenite and geikielite Raman spectra acquired on Bruker's BRAVO spectrometer. Spectra are color-coded based on %ilmenite content, where pure $Fe^{2+}TiO_3$ is represented with yellow and pure $MgTiO_3$ with purple.

This is the peer-reviewed, final accepted version for American Mineralogist, published by the Mineralogical Society of America.
The published version is subject to change. Cite as Authors (Year) Title. American Mineralogist, in press.
DOI: https://doi.org/10.2138/am-2023-9262. http://www.minsocam.org/

Table 1. Raman peak positions and modes of geikielite and ilmenite for our dataset compared to the literature.

Raman Peak Positions (cm^{-1})				Raman Modes	
geikielite		ilmenite		Wang et al., 2004; Okada et al., 2008	
this study	Linton and Navrotsky, 1999	this study	Wang et al., 2004		
306	306	-	333	E_g	translation
327	327	370	368	A_g	translation
352	352	-	-	A_g	bending
397	397	-	-	E_g	bending
485	485	-	-	E_g	bending
-	502	-	-	A_g	bending
640	641	-	-	E_g	stretching
715	714	681	683	A_g	stretching

Note: Two additional Raman modes are predicted and observed outside the wavenumber range of the Raman instrument utilized in this investigation.

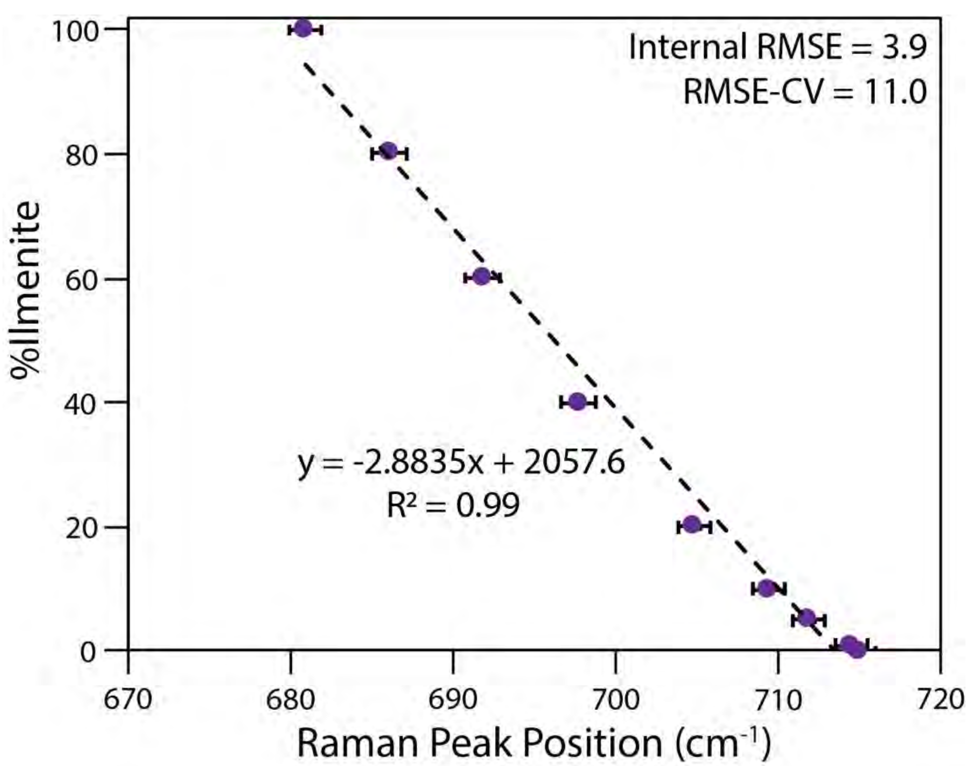

Figure 2. Univariate model of %ilmenite versus Raman peak position (cm^{-1}) of the diagnostic Raman feature between ~681 – 715 cm^{-1} (A_g) with error bars of the gaussian peak fit. The linear model, R^2 value, internal RMSE, and RMSE-CV are reported.

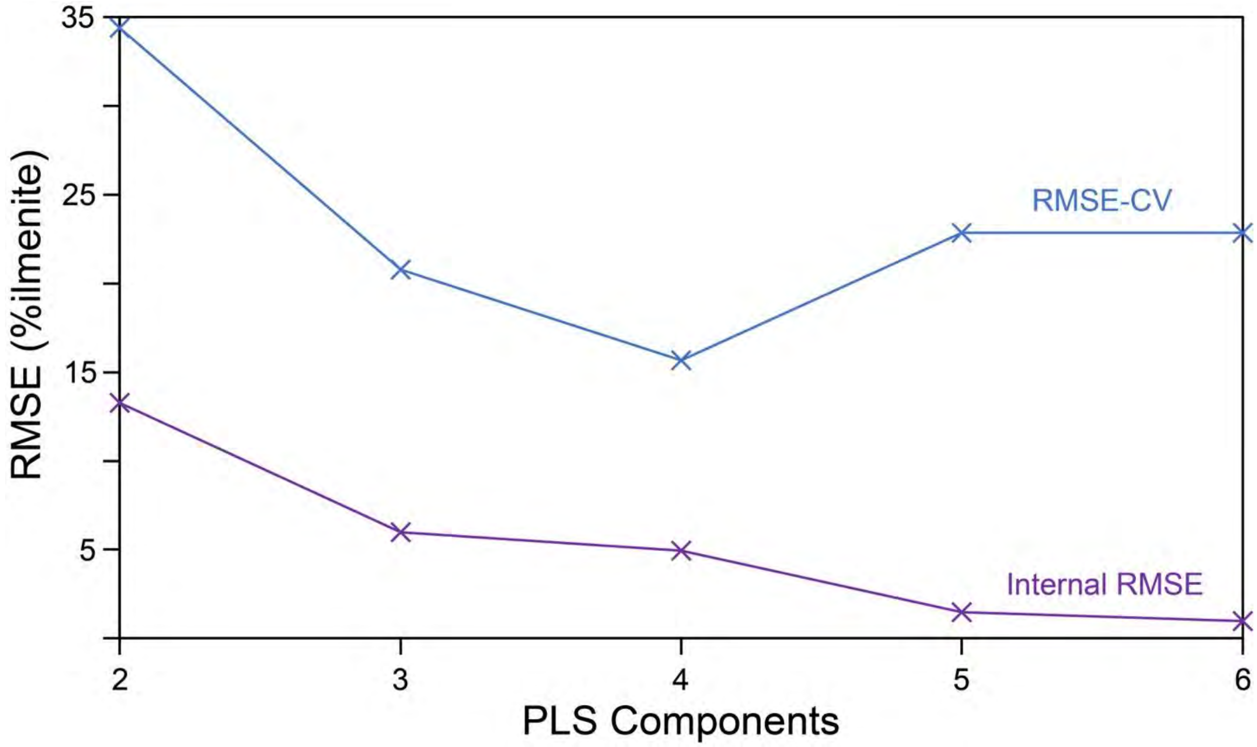

Figure 3. Multivariate model errors (internal RMSE and RMSE-CV) for 2 – 6 PLS model components.